ELSEVIER

Deep-Sea Research II 52 (2005) 627–650

DEEP-SEA RESEARCH
PART II

www.elsevier.com/locate/dsr2

Discrete eddies in the northern North Atlantic as observed by looping RAFOS floats

D.R. Shoosmith[a,*], P.L. Richardson[b], A.S. Bower[b], H.T. Rossby[c]

[a]*Department of Meteorology and Physical Oceanography, Rosenstiel School of Marine and Atmospheric Science, University of Miami, 4600 Rickenbacker Causeway, Miami, FL 33149-1098, USA*
[b]*Physical Oceanography Department, Woods Hole Oceanographic Institution, MS#21, Woods Hole, MA 02543, USA*
[c]*Graduate School of Oceanography, University of Rhode Island, Narragansett, RI 02882, USA*

Received 14 April 2004; accepted 1 December 2004

Abstract

RAFOS float trajectories near the 27.5 density level were analyzed to investigate discrete eddies in the northern North Atlantic with the objective of determining their geographical distribution and characteristics. Floats that made two or more consecutive loops in the same direction (loopers) were considered to have been in an eddy. Overall 15% (24 float years) of the float data were in loopers. One hundred and eight loopers were identified in 96 different eddies. Roughly half of the eddies were cyclonic (49%) and half were anticyclonic (51%), although the percentages varied in different regions. A few eddies were quasi-stationary for long times, one for over a year in the Iceland Basin, and many others clearly translated, often in the direction of the general circulation as observed by non-looping floats. Several floats were trapped in eddies in the vicinity of the North Atlantic Current just upstream (west) of the Charlie Gibbs (52°N) and Faraday (50°N) Fracture Zones, which seem to be preferred routes for flow crossing the Mid-Atlantic Ridge. Five floats looped in four anticyclones that translated southwestward away from the eastern boundary near the Goban Spur (47–50°N). These could have been weak meddies forming from remnants of warm salty Mediterranean Water advected northward along the eastern boundary.

1. Introduction

Due to the difficulty in following discrete eddies, their life histories and trajectories are poorly known in many parts of the ocean. This is especially true of interior or subsurface eddies. During the last few years numerous freely drifting neutrally buoyant RAFOS floats launched into the northern North Atlantic (Furey et al., 2001; Anderson-Fontana et al., 2001) became trapped and looped for various lengths of time in discrete eddies providing new information about them. This study systematically identifies floats that

*Corresponding author. Tel.: +1 305 421 4011; fax: +44 0 870 1384896.
E-mail address: dshoosmith@rsmas.miami.edu (D.R. Shoosmith).

0967-0645/$ - see front matter © 2005 Elsevier Ltd. All rights reserved.
doi:10.1016/j.dsr2.2004.12.011

looped in what are interpreted as being discrete eddies. Results reveal new information concerning their number, distribution and trajectories.

When a float becomes trapped in the rotating swirl flow around an eddy's center, the path of the eddy itself can be inferred from the float trajectory. Thus a single float trajectory becomes representative of a huge mass of water translating with the eddy. Additional information obtained from float trajectories includes the size of eddies, their rotation rates, and swirl speeds. Information about eddies is important because they are thought to play a leading dynamical role in the general circulation. The long lifetimes and long displacements of some eddies suggest they can be an important transport mechanism in the ocean.

The data set considered here consists of 116 floats tracked as part of the World Ocean Circulation Experiment (WOCE) Atlantic Circulation and Climate Experiment (ACCE) (Fig. 1). The floats were deployed across the North Atlantic Current-subpolar frontal region between (generally) 45–55°N near 35°W (80% of the floats) and in the Mediterranean Water along the eastern boundary between 48°N and 54°N (20% of the floats). The purpose of the experiment was to study the northward flow of warm subtropical water into the subpolar gyre and Nordic Seas. The emphasis of the RAFOS program discussed here is the North Atlantic Current as it flows eastward along the subpolar front, which is located near 50°N in the central Atlantic, and its downstream pathways. Along and across this front warm subtropical water makes its way into the subpolar region, possibly augmented by warm Mediterranean Water via a poleward eastern boundary current (see e.g., Reid, 1978; McCartney and Mauritzen, 2001). An important issue is the role of eddies, as opposed to the mean flow, in the northward flux of heat and salt.

The floats were deployed on six cruises between November 1996 and July 1998 and were tracked up to January 2000. None were intentionally launched in eddies. Most float missions were 18–24 months long. The floats were isopycnal-following and were ballasted for the 27.5 sigma-t surface, which extends from around 900 m in the Mediterranean Water near the eastern boundary upwards across the subpolar front to less than 100 m in the Irminger and Labrador Basins (where it outcrops in winter). All floats measured temperature and pressure daily (some measured dissolved oxygen, see Anderson-Fontana et al., 2001), and daily positions were obtained by acoustic tracking. The daily positions provide sufficient resolution to resolve details of the eddy variability. More information about the tracking and float data is provided in data reports published by Furey et al. (2001) and Anderson-Fontana et al. (2001). Other results of the float program have been given by Bower et al. (2000), Rossby et al. (2000), and Bower et al. (2002).

2. Methods

Each float trajectory was visually examined for loops and cusps, which reveal the characteristic motion of a particle in an eddy, a swirl velocity around the eddy center plus its translation. Time series of velocity, temperature and pressure were studied to help estimate when a float entered and exited an eddy. An eddy was defined by two or more consecutive loops in the same direction (looper) within a float trajectory. This definition attempts to isolate discrete eddies (i.e. coherent vortices), with their approximately symmetric and rotational circulation and a volume of trapped fluid that translates with the eddy, from other types of non-stationary fluid motion (Paillet, 1999; Richardson, 1993). Identifying eddies from trajectories is clearly subjective, and there remains the possibility that some eddies were mis-identified. Numerous floats looped many times similar to loopers in eddies that have been well documented by a variety of techniques, suggesting that our loopers are indicative of real discrete eddies (see e.g., references by Bower, Paillet, Pingree and Richardson).

Once the individual loopers were identified, they were checked to determine if more than one float looped in the same eddy. Eddies were then segregated into cyclones and anticyclones and ordered by the maximum number of loops in each eddy (see appendices). The number of loops was estimated visually from the float trajectories and

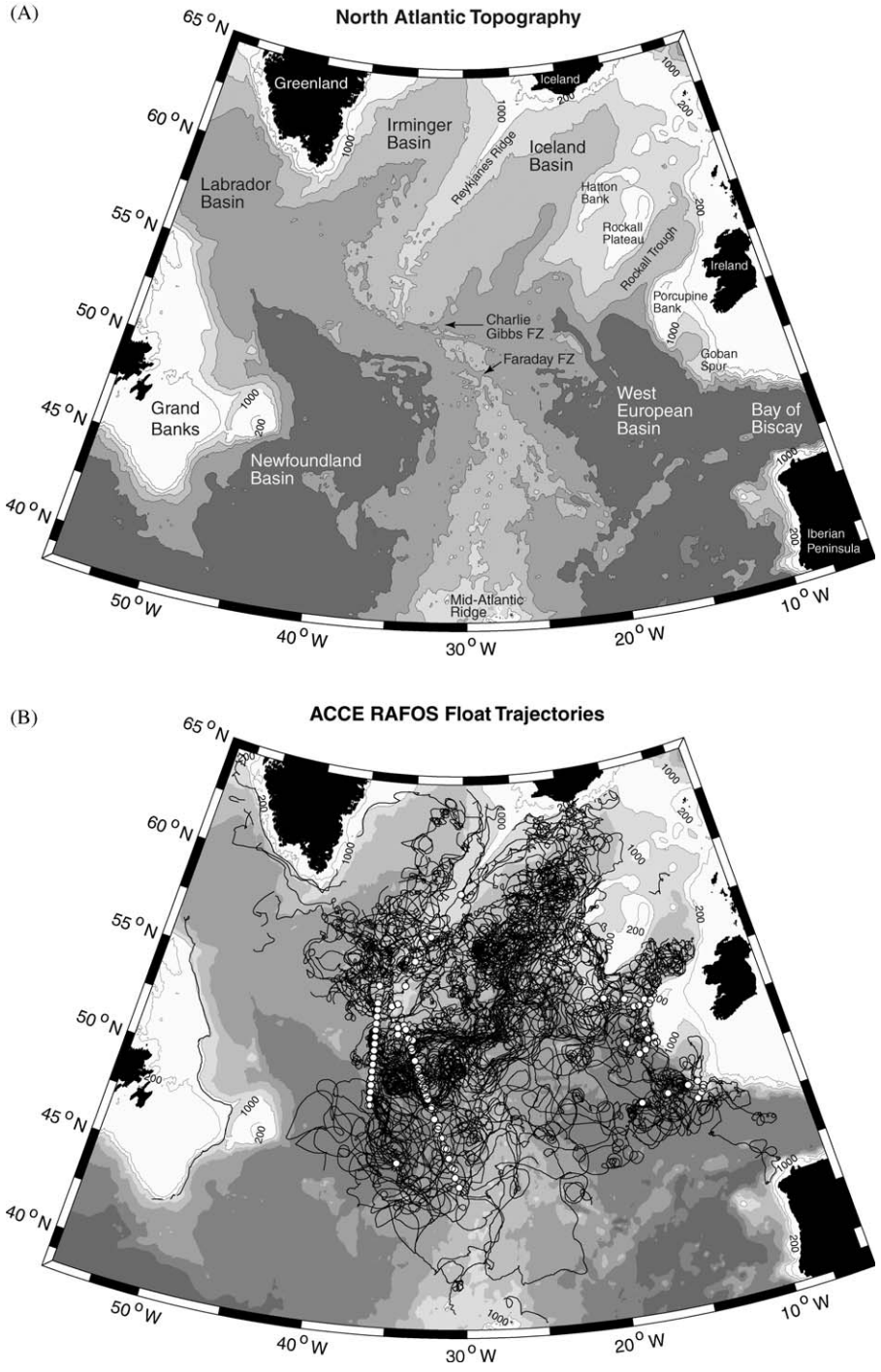

Fig. 1. (A) Topographic features in the North Atlantic. (B) One hundred and thirteen RAFOS float trajectories centered near the 27.5 density layer. Floats launched (small circles) near 37°W were by University of Rhode Island (URI); those launched over the Mid-Atlantic Ridge and near the eastern boundary were by Woods Hole Oceanographic Institution (WHOI). Floats launched in the North Atlantic Current tended to drift northeastward and floats launched along the eastern boundary tended to drift northwestward north of Porcupine Bank (52°N) and southwestward south of Porcupine Bank. Many floats drifted in a counter-clockwise sense around the Iceland Basin and clockwise around the Reykjanes Ridge and into the Irminger Basin.

used to estimate the period of rotation (T) by dividing the days tracked by the number of loops. The characteristic swirl speed (V_s) was estimated as being equal to the root mean square (RMS) velocity of the float about its mean velocity (U in the east direction and V in the north direction) averaged over each looper series. The mean diameter (D) was estimated from the mean looping period (T) and mean swirl speed (V_s) with the relation $D = V_s T/\pi$. Rossby number Ro was calculated by dividing the relative vorticity of an eddy ζ by the planetary vorticity f, $Ro = \zeta/f$. The relative vorticity ζ was estimated as being two times the rotation rate, ω (which was calculated from the looping period $\omega = 2\pi/T$), assuming solid body rotation. If a float was located outside the (approximately) solid body rotation core region of an eddy, then the calculated Rossby number could be an overestimate. Since the period of rotation and swirl speed vary with radius, these characteristics estimated from the floats are representative of the radius sampled by the floats. This should be kept in mind when comparing characteristics of different eddies.

The radial variation of swirl velocity was calculated and plotted for three representative eddies (AC1, AC3 and C12) whose trajectories included a large number of well-resolved loops. The daily float positions were smoothed using a simple filter of length equal to the eddy period, giving the daily mean eddy-center position. The radius of the float was then obtained by subtracting the mean eddy position (smoothed series) from the original data. Swirl velocity was calculated from the angular velocity and radius of the float.

3. Results

Of the 113 float trajectories analyzed, 69 (61%) floats looped in eddies at some time. Of the total 160 float years of data, 24 float years are looping records. This amounts to 15% of the data and is consistent with results of an analysis of eddies in hydrographic data from the same region (Paillet, 1999) and from a study of float data located farther south in the North Atlantic (Richardson, 1993).

One hundred and eight individual loopers were identified in 96 unique eddies, 49 anticyclones and 47 cyclones (Fig. 2, appendices). Therefore approximately half (51%) of the loopers were anticyclones and half (49%) cyclones. Fifty-nine percent of the daily looping records were in anticyclones, and an average anticyclone looper was 95 days long, considerably longer than an average cyclone looper of 72 days. The five longest looper records were all anticyclones and ranged from 251 to 502 days.

Fig. 3 and Table 1 show some geographical differences in the distribution of eddies encountered. The highest percentage of anticyclones (63%) was found in the West European Basin, where 20% of the total number of eddies was observed. This may be due to the presence of a northward-flowing eastern boundary current (Pingree and Le Cann, 1992a, b) which could preferentially shed anticyclones from offshore meanders. Two of the five longest anticyclone records (261 and 502 days) began near the eastern boundary in this area. The Newfoundland Basin contained 27% of the eddies, 62% of which were cyclones, the largest percentage of any area. This may be because much of the area lies east and south of the mean position of the North Atlantic Current axis and because southward meanders and cut-off pieces of them would tend to be cyclonic. Two long anticyclone records (251 and 271 days) were also measured in this area in a quasi-stationary eddy. Thirty-nine percent of the eddies were measured in the Iceland Basin and Rockall Trough, almost equally split between cyclones and anticyclones. On average these looper records are 66 days long, much shorter than the average in other areas except for the Irminger Basin. However, the second longest anticyclone record, 336 days, was found in this region in a quasi-stationary eddy.

Fig. 2. Looping float trajectories in anticyclones (A) and cyclones (B), starting with a small circle. Each looping float made two or more consecutive loops in the same direction. One hundred and eight loopers were identified in 96 different eddies, 49 anticyclones and 47 cyclones. Each looper is labeled with an eddy identification number followed by a float number.

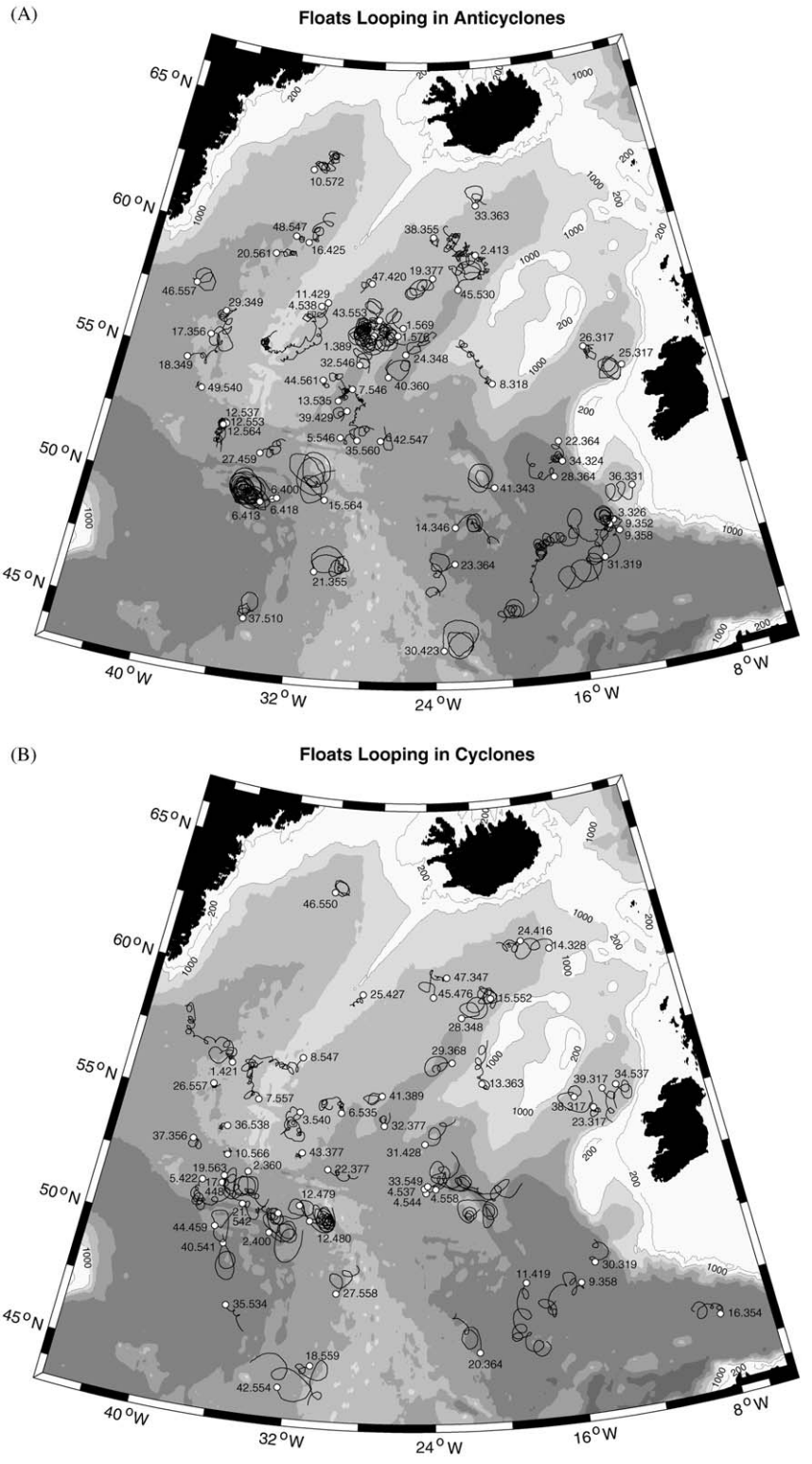
(A)
Floats Looping in Anticyclones
65 °N
60 °N
55 °N
50 °N
45 °N
40 °W
32 °W
24 °W
16 °W
8 °W
10.572
33.363
48.547
16.425
20.561
38.355
2.413
47.420
19.377
45.530
46.557
29.349
11.429
4.538
43.553
1.569
1.578
17.356
1.389
32.546
24.348
18.349
26.317
25.317
49.540
44.561
7.546
40.360
8.318
13.535
12.537
12.553
12.564
39.429
5.546
42.547
35.560
22.364
27.459
34.324
28.364
36.331
6.400
6.418
6.413
15.564
41.343
3.326
9.352
9.358
14.346
31.319
23.364
21.355
37.510
30.423
(B)
Floats Looping in Cyclones
65 °N
60 °N
55 °N
50 °N
45 °N
40 °W
32 °W
24 °W
16 °W
8 °W
46.550
24.416
14.328
47.347
25.427
45.476
15.552
28.348
8.547
29.368
1.421
13.363
39.317
34.537
26.557
7.557
41.389
6.535
3.540
38.317
23.317
36.538
37.356
32.377
10.566
43.377
31.428
2.360
22.377
19.563
5.422
33.549
4.537
4.544
4.558
12.479
44.459
12.480
40.541
2.400
30.319
11.419
9.358
27.558
35.534
16.354
18.559
20.364
42.554

Whilst these results detail the number of eddies encountered in each region, there is likely to be a bias due to the uneven distribution of float records (see Fig. 1). To gain a measure of this bias, we calculate the likelihood of encountering an eddy (P_e), defined by the average number of eddies found per float year of data (Fig. 3 and Table 1). This calculation reveals that although fewest eddies were found in the Irminger Basin (14), the region actually has the highest number of eddies per float measurement ($P_e = 0.86$). It is closely followed by the Iceland Basin ($P_e = 0.77$), where the highest number of eddies (37) was found. The Newfoundland Basin actually has the lowest P_e (0.47) in spite of the large number of eddies found here. This is most likely due to the large number of floats launched in this region.

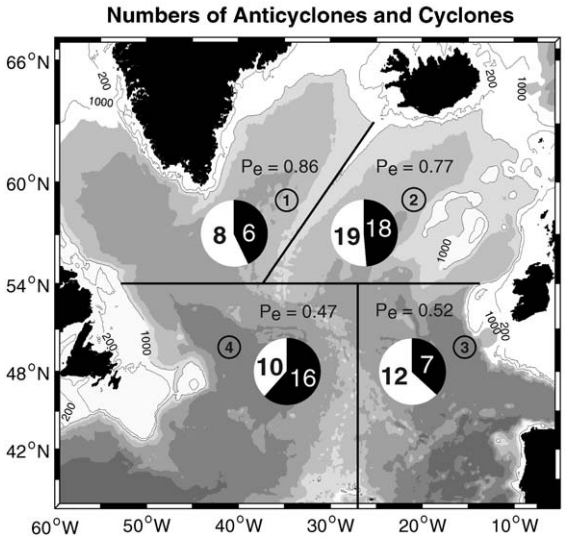

Fig. 3. Numbers of anticyclones (white segments) and cyclones (black segments) in four areas of the North Atlantic. The likelihood of encountering an eddy (P_e), defined as the average number of eddies found per float year of data, is also shown (see Table 1).

Four anticyclones and three cyclones had more than one float looping in them (Fig. 4). Three of these (C4, AC6, AC12) occurred because floats were launched very close together in both space and time.

Some eddies clearly translated and others look like they remained quasi-stationary. By quasi-stationary we mean that the center of the eddy as inferred from float loops moved somewhat but that the net displacement was small. Considering the sometimes erratic behavior of eddies, long records are required to fully document eddy

Table 1
Rotation direction of records and eddies in four areas in the North Atlantic (shown in Fig. 3)

	Area 1 Irminger Basin North of 54°N, West of MAR	Area 2 Iceland Basin, Rockall Trough North of 54°N, East of MAR	Area 3 West European Basin South of 54°N, East of 27°W	Area 4 Newfoundland Basin South of 54°N, West of 27°W	Entire Area
Total no. of records	5,977	17,673	13,596	21,082	58,328
Total no. of float-years	16.4	48.4	37.2	57.8	159.8
Records that are looping (%)	15.0	13.9	20.3	12.3	14.9
Looping records that are AC/C (%)	60.2/39.8	62.3/37.7	61.9/38.1	53.7/46.3	59.4/40.6
Total no. of loopers	14	39	22	33	108
No. of loopers that are AC/C	8/6	21/18	13/9	14/19	56/52
Total no. of eddies	14	37	19	26	96
No. of eddies that are AC/C	8/6	19/18	12/7	10/16	49/47
Eddies that are AC/C (%)	57.1/42.9	51.4/48.6	63.2/36.8	38.5/61.5	51.0/49.0
No. of eddies as a % of total	14.6	38.5	19.8	27.1	100
No. of eddies per float-year of data (P_e)	0.86	0.77	0.52	0.47	2.62

Areas 1 and 2 have as their common east-west boundary a line running down the centre of the mid-Atlantic ridge, described by $y = (0.741x) + 81.85$, where y is latitude and x is longitude, which intersects 54°N at 37.6°W. MAR = Mid Atlantic Ridge, AC = anticyclones, C = cyclones.

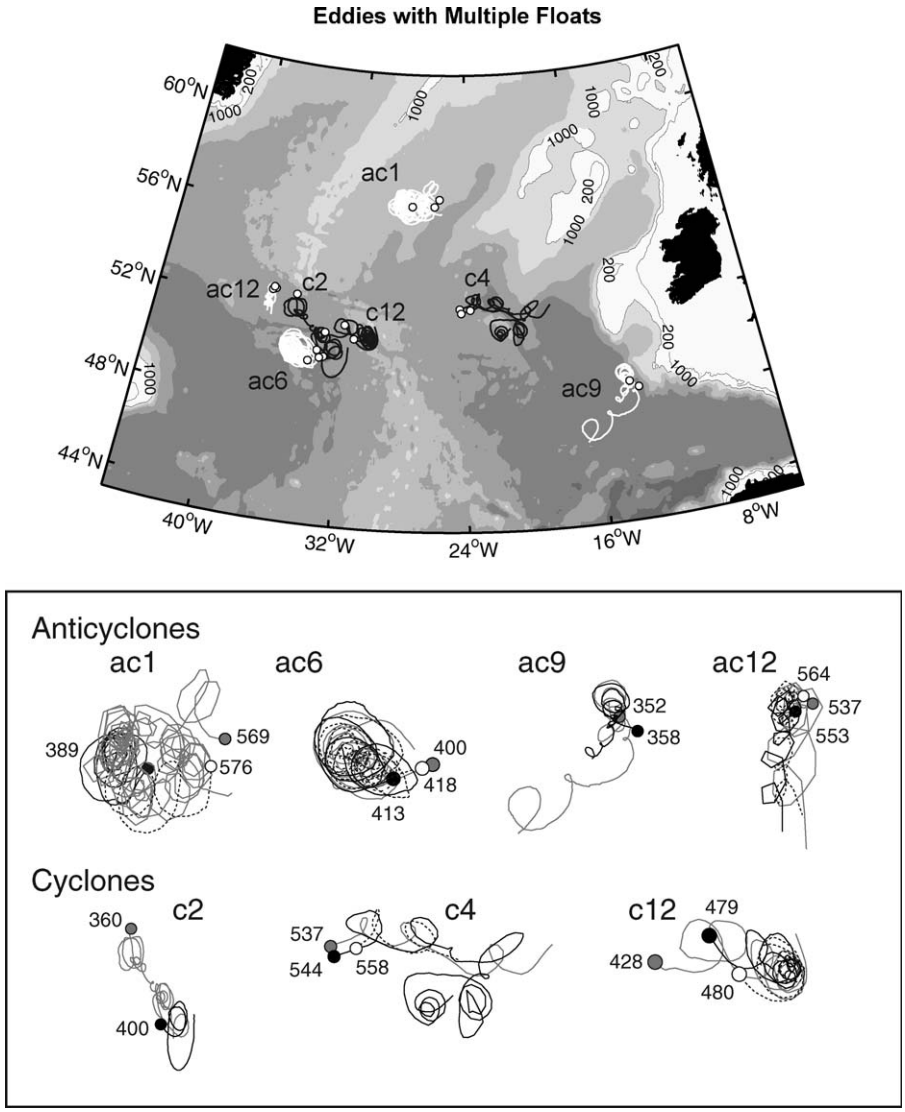

Fig. 4. Eddies with more than one float looping in them. Top panel shows the eddy locations. Bottom panel shows different float trajectories in each eddy. Anticyclones AC1 and AC6 remained quasi-stationary for long periods of time, 14 months for AC1 near 57°N 28°W in the Iceland Basin and 9 months for AC6 near 50°N 35°W in the North Atlantic Current. The other eddies appeared to translate.

trajectories. Unfortunately, long looping records are sparse and therefore many loopers are needed to give a reasonable indication of typical eddy translation. We estimated eddy translation for records of at least 30 days in length and containing at least three loops (Fig. 5). Eddies that looked quasi-stationary were omitted from Fig. 5, which shows displacement vectors of 42 translating eddies. In general the translation of eddies appears to follow the mean circulation as estimated by using all available RAFOS float trajectories to objectively map the flow field (Fig. 6).

Rossby number was calculated for each looper, and based on histograms (not shown), *Ro* appears to be quite symmetrical around $Ro = 0$ with a clear cut-off at a magnitude of 0.3. This is due to

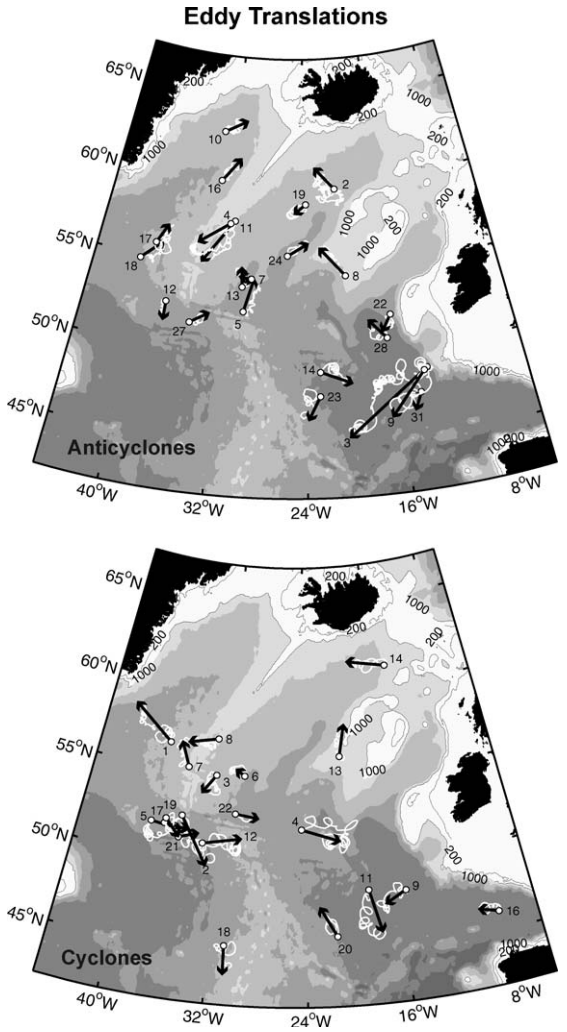

Fig. 5. Displacement vectors of translating eddies using records of at least 30 days and three loops. Eddy numbers are indicated. Eddy translations are due to (i) self-advection, (ii) advection by background currents (as indicated by non-looping floats) which often appear to be constrained by sea floor topography, and (iii) interactions with other eddies. A few eddies remained nearly stationary for long times in the Iceland Basin and west of the Mid-Atlantic Ridge near the Charlie Gibbs and Faraday Fracture Zones (see Fig. 2).

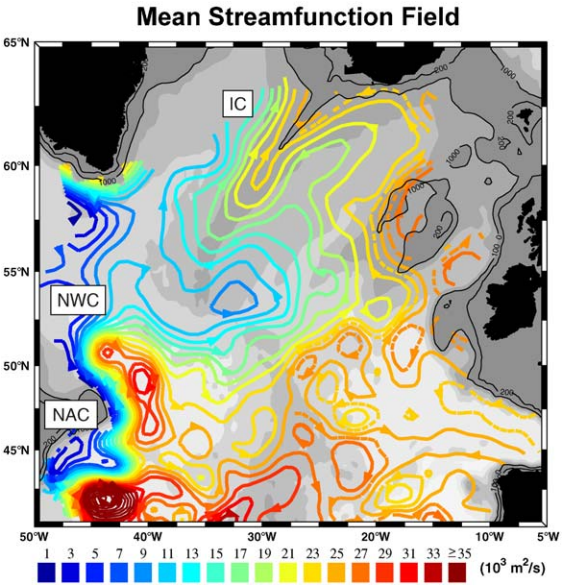

Fig. 6. Mean streamfunction field for the subpolar North Atlantic based on subsurface RAFOS float data near a 27.5 density layer (from Bower et al., 2002). The data used to construct this figure include float trajectories shown in Fig. 1 as well as contributions from additional experiments amounting to a total of 243 float years. The color bar indicates volume transport for a 1-m thick layer. NAC indicates the North Atlantic Current, NWC the Northwest Corner and IC the Irminger Current.

temporal limitations of the daily float time series, which are not able to resolve eddies with periods of rotation shorter than two days, $Ro \sim 0.6$. The practical maximum magnitude of *Ro* is around 0.3 because we only included floats that clearly looped, and these series consisted of at least 3–4 positions (days) per loop.

Ro was plotted as a function of the variables given in the appendices in order to identify trends. Since there did not appear to be obvious differences in the distributions of *Ro* for cyclones and anticyclones, absolute values are discussed below. *Ro* increases with latitude from roughly 0.05 in the south to 0.15 in the north (Fig. 7). This is due to the period of rotation, which decreases with latitude faster than f increases, and also corresponds to an increase of swirl speed with latitude since the looping diameter turned out to be roughly constant with latitude. *Ro* increases towards the west in the southern region ($<54°$N), also corresponding to a decrease of period and increase of swirl speed there. The lowest values of *Ro* tend to be located in the southeastern region, corresponding to large looping periods and low swirl speeds. This overall

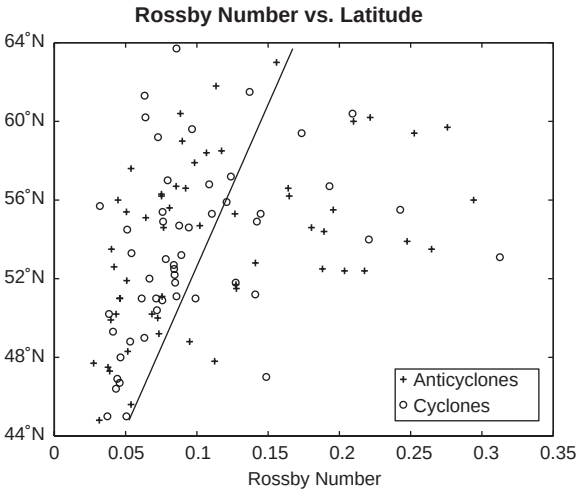

Fig. 7. Rossby number versus latitude for cyclones and anticyclones. A line of best fit (using the least squares method) giving Rossby Number as a function of latitude is shown.

pattern resembles the geographical distribution of eddy kinetic energy based on all the float data (not shown) and other studies (e.g., Fratantoni, 2001; Heywood et al., 1994).

Two other trends were found. The first, related to the geographical trends, is that *Ro* increases with swirl speed. The second is that *Ro* decreases with diameter. This is a result of the clear trend of increasing looping period with eddy diameter and indicates that the larger diameters of eddies rotate more slowly than smaller diameters, which could be either observations of smaller eddies or the inner portions of larger eddies.

Detailed results of the eddy study are discussed below grouped into the different geographical regions, starting with the North Atlantic Current west of the Mid-Atlantic Ridge, and then following the flow into the Iceland Basin, around the Reykjanes Ridge and into the Irminger Basin. Finally, eddies in the West European Basin will be described.

3.1. North Atlantic Current west of the Mid-Atlantic Ridge

The area upstream (west) of where the North Atlantic Current (NAC) crosses the Mid-Atlantic Ridge (50–52°N) is abundant with eddies (Fig. 2), some translating generally eastward (Fig. 5), but three appear to be quasi-stationary (AC6, AC15, C12). A time sequence of the looping trajectories is shown in Fig. 8. By the end of October 1997 three floats were trapped in anticyclone AC6, which remained near 50°N 35°W for at least 9 months, positioned over slightly higher topography than its surroundings. Some large loops suggest an overall diameter of around 150 km for this anticyclone. Maximum swirl speeds were around 15–20 cm/s near a diameter of 50 km. Fastest loops had a period of rotation around 10 days and a *Ro* of −0.13.

During the 9 months AC6 was tracked, floats looped in seven cyclones in the area surrounding AC6. In March 1998 cyclones C2 and C5, which had been relatively stationary for the preceding 2 months, translated eastward around the periphery of AC6 as though they were being advected by the swirl velocity of AC6. AC6 and C2 were close for at least 4 months and possibly interacting as indicated by a float, which left AC6 and immediately entered C2. Another case of two close eddies forming a dipole-like structure were AC12 and C19 in July 1998 near 52°N 37°W. In September 1998 cyclones C19 and C21 translated southeastward near where C2 did so 6 months earlier. The trajectories of some background floats imply that AC6 could have still been present at that time although no floats looped in AC6 then.

Cyclone C12 was tracked with three floats for 5.3 months starting in late October 1997; during the first 2 months it translated southeastward around 150 km but then remained quasi-stationary for the next 3 months near 51°N 31°W and the western edge of the Mid-Atlantic Ridge crest. The swirl velocities of cyclone C12 appear to be a linear function of radius (Fig. 9B), which suggests that the core of the eddy was in solid body rotation with a period of 9 days ($Ro = 0.14$) near a depth of 430 m and 15 days ($Ro = 0.09$) near 550 m. The two floats at different depths indicate considerable vertical shear, with fastest swirl velocities at any given radius located at the upper level, near 430 m. The location of C12 is close to the spot where anticyclone AC15 later remained quasi-stationary for 5.6 months (January–June 1999).

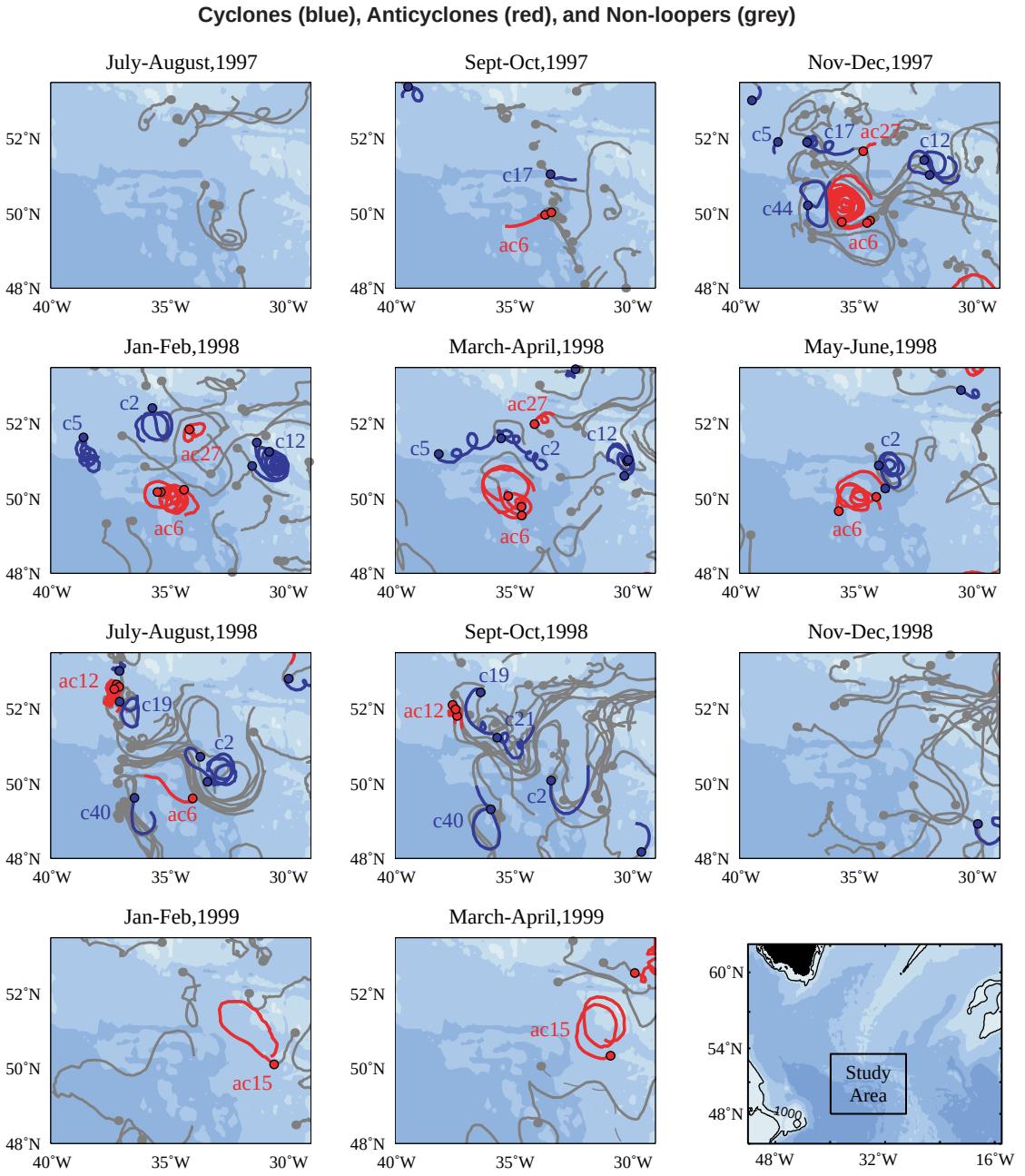

Fig. 8. Floats looping in anticyclones (red) and cyclones (blue) in the vicinity of the NAC just upstream of the Mid-Atlantic Ridge, as shown in the final panel. Floats were launched just before July 1997, in October and November 1997 and in July 1998. Non-looping float trajectories are added to show the background flow field in the vicinity of the eddies. By the end of October 1997, three floats became trapped in quasi-stationary anticyclone AC6 near 50°N 35°W which lasted for at least 9 months, positioned over slightly higher topography than its surroundings. In March 1998 cyclones C2 and C5 translated eastward around the perimeter of the anticyclone as though they were advected by the larger eddy's swirl velocity. In late July 1998 anticyclone AC12 and cyclone C19 formed a dipole near 52°N 37°W.

This anticyclone also had some large 140 km diameter float loops. These quasi-stationary eddies appear to be somewhat anomalous compared to the more general pattern of translating eddies.

A summary of all the float trajectories in this region, Fig. 8, gives a good picture of the complicated flow field in and around the eddies during a 2-year period and suggests a possible explanation of why the eddies were quasi-stationary. Groups of floats drifting eastward in the NAC appear to have been advected around the periphery of several of the eddies tracked with looping floats (AC6, C2, C19, C21), indicating the close connection between bands of flow within the NAC and the closed circulation in the eddies. Particularly striking is the way several floats made a 200 km diameter partial loop around the periphery of C2 during July and August 1998 (Fig. 8). Trajectories of some background floats suggest the presence of additional eddies that do not contain any loopers. Throughout the sequence of bi-monthly frames floats can be seen heading toward and passing over the Charlie Gibbs Fracture Zone located near 52°N and, to a lesser extent, the Faraday Fracture Zone near 50°N, showing these as preferred routes for flow crossing the

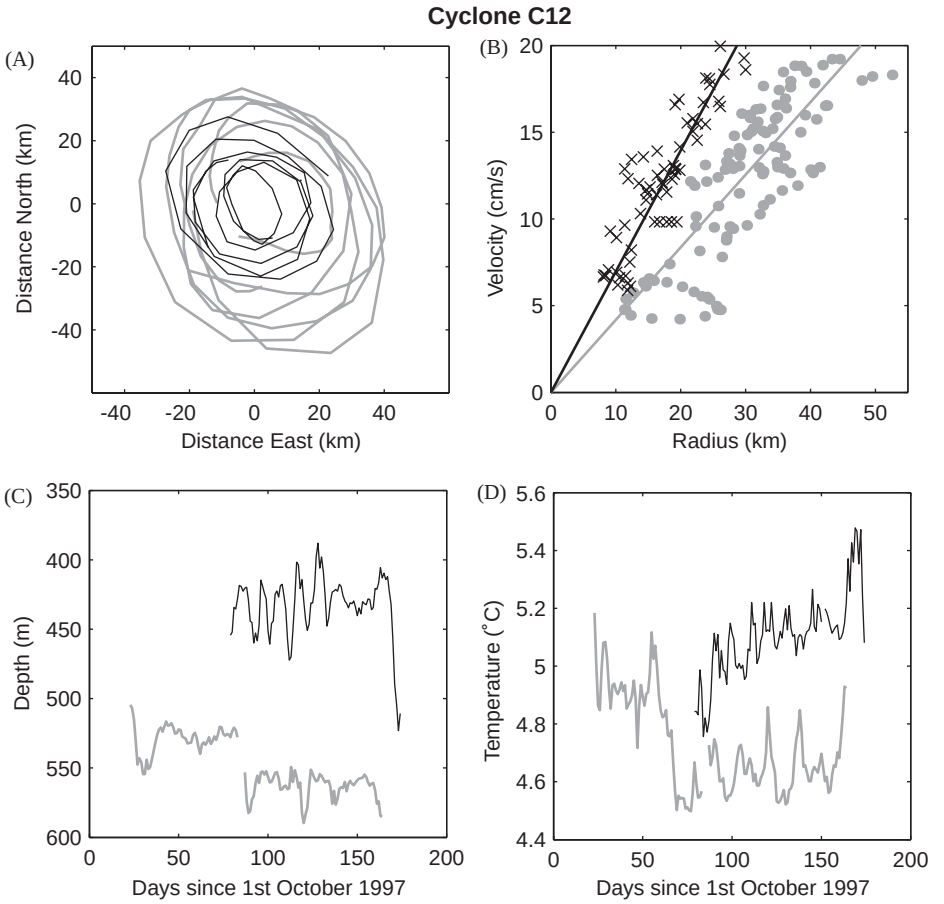

Fig. 9. Cyclone C12 on the western flank of the Mid-Atlantic Ridge, as measured by floats 428 (gray) and 479 (black): (A) float position relative to the eddy center as calculated by subtracting the mean eddy position from the float position; (B) variation of swirl velocity with radius, with lines corresponding to periods of 15 days (gray) and 9 days (black); (C) variation of depth and (D) variation of temperature measured by the two floats.

Mid-Atlantic Ridge. East of the Ridge the float trajectories remained generally clustered in the two branches as indicated schematically in Fig. 6. The funneling of floats over the fracture zones illustrates the influence of the 3000 m deep gaps on the thermocline-level flow field above. The implication is that the NAC is constrained by sea-floor topography in this region.

These observations suggest that the sea-floor topography could cause the quasi-stationary behavior of the eddies. One possible scenario is that over and just west of the Mid-Atlantic Ridge the NAC is constrained by sea-floor topography to flow in particular quasi-stationary meanders in which are embedded quasi-stationary eddies. This would be analogous to the quasi-stationary meanders and eddies of the NAC farther west where it flows northward adjacent to the western boundary off the Grand Banks of Newfoundland (Rossby, 1996; Dutkiewicz et al., 2001). An alternative scenario, but one we think less likely, is that the quasi-stationary eddies are particularly intense and deep reaching ones which are trapped by the sea floor of the western Ridge flank and deflect the generally eastward flow field of the NAC around them. It should be noted that Agulhas Current rings have been observed to pass westward over the Walvis Ridge, which rises above 1000 m and over the deeper ~2000 m Mid-Atlantic Ridge (Byrne et al., 1995; Schouten et al., 2000; Richardson and Garzoli, 2003), which supports the first scenario. There is only weak background current (the Benguela Current) in the vicinity of the ridges where the Agulhas rings pass over, unlike the swifter NAC flowing over the Mid-Atlantic Ridge. Presumably the full 3-D flow field of the NAC, which includes deep reaching eddies, interacts with the Ridge topography, and thus the first scenario is probably more relevant.

3.2. Iceland basin

Most eddies in the Iceland Basin translated in a counter-clockwise sense around the Basin (Fig. 5) following the main flow of the general circulation as measured by floats (see Fig. 6): northwestward across the southern Rockall-Hatton Plateau (AC8), northward along the western edge of this plateau (C13, AC24), counter-clockwise around the northern part of the basin (C14, AC2), southwestward along the east side of the Reykjanes Ridge (AC4, AC11), westward over the Mid-Atlantic Ridge near 56°N (C7, C8). The mean velocity (and standard error) of these nine eddies along the path described above is 2.7 cm/s ($\pm$0.5 cm/s).

One long-lasting quasi-stationary eddy (AC1) stands in strong contrast to these translating eddies. Anticyclone AC1, the second longest tracked eddy of the experiment, was observed for 15.4 months, from October 1998 to November 1999 near the central part of the Iceland Basin near 56.5°N 28.0°W (Fig. 10). Float 389 looped in AC1 during October 1998–January 1999. In mid-December 1998 float 569 became caught and looped in an anticyclone near 57°N 26°W, which translated toward AC1 and appears to have merged with it in January 1999, at which time float 389 ceased looping (Fig. 10). In August 1999 float 576 was entrained into AC1 and looped until September 1999. The three float trajectories show that AC1 remained within about 50 km of its mean position during the 14 months. During the first six months AC1 moved little, but during the last eight months the center of AC1 appears to have made a clockwise loop roughly 100 km in diameter. The overall size of AC1 estimated from the largest loops is around 100 km. Float 569 made a total of 46 loops, the largest number of any eddy, with a mean period of rotation of 7.3 days and a *Ro* of −0.16. The float spent three months at a mean depth of 440 m and then rose to 60 m (Fig. 11A) on March 20th, which we infer was due to the upper well-mixed layer reaching down to 400 m. After a further 2.5 months the float subsided to 200 m, where it stayed for the remainder of its time in eddy AC1, 5.3 months. Below a depth of 125 m, the majority of the loops were well behaved and these are shown in Fig. 11B. Swirl velocities of AC1 within a radius of 35 km appear to lie close to a line of constant period 6.5 days (Fig. 11C), indicating solid-body rotation, with a *Ro* of −0.18. Fastest swirl speeds were around 35 cm/s near a depth of 400 m and diameter of 60 km.

The reason the eddy remained quasi-stationary is unknown. There do not appear to be major

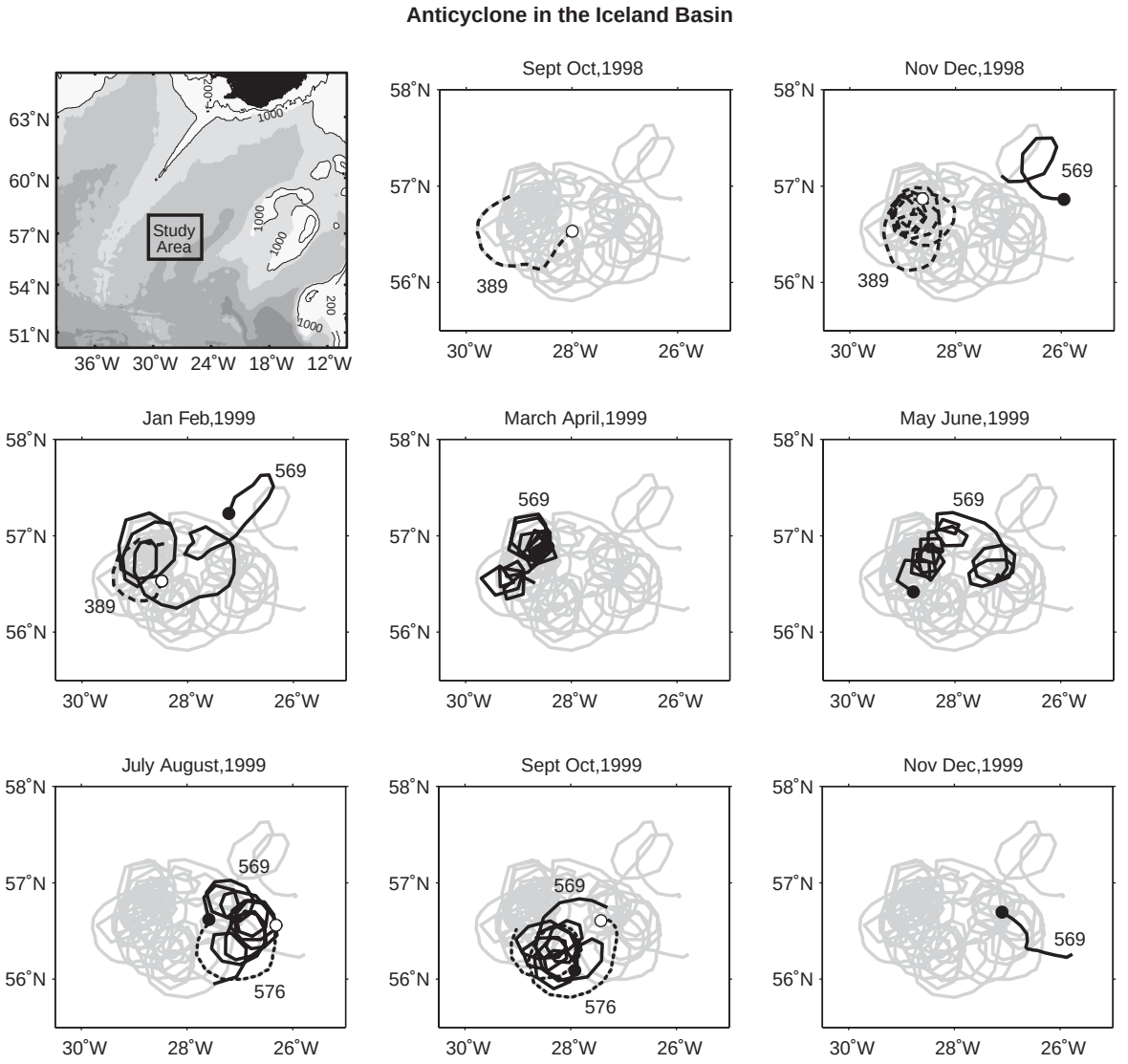

Fig. 10. Two-month time frames showing three floats (389, 569, 576) looping in anticyclone AC1 in the Iceland Basin. The beginning of each trajectory is marked with a small circle. This anticyclone is the second longest one tracked at 14 months. During this time it remained within ~50 km of its mean position.

topographic features below it that could constrain the eddy (or nearby flow) to such a spot. The eddy lies along the axial center of the counter-clockwise circulation within the Iceland Basin as measured by floats (Bower et al., 2002): northward flow east of AC1, southwestward flow west of AC1 and northwestward flow south of it. The mean flow field at the anticyclone's location appears to be weak but might counter the eddy self-induced advection, which would tend to be southward for a barotropic anticyclone (southwestward relative to local f/H contours that are directed in a northeast-southwest direction) (Nof, 1981, 1983; Cushman-Roisin et al., 1990).

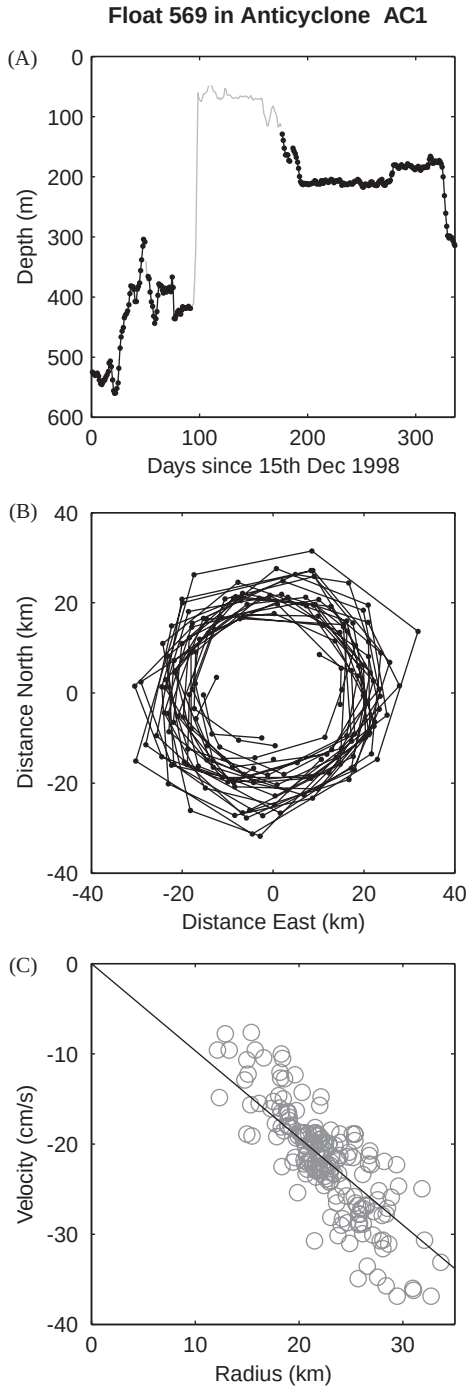

Fig. 11. Eddy AC1 in the Iceland Basin, as measured by float 569: (A) float depth over the duration of the looping trajectory, with data used in (B) and (C) shown as black dots; (B) float position relative to the eddy center; (C) variation of swirl velocity with radius, with the line corresponding to a period of 6.5 days shown in black.

We note that other rather similar quasi-stationary eddies have been observed in the Iceland Basin. For example the PRIME eddy (Martin et al., 1998; Wade and Heywood, 2001) was an anticyclone located near 59°N 21°W that remained nearly stationary from late 1995 to mid-1996. The eddy was in the shape of a 120 km diameter lens, centered around 600–700 m in depth, and had a significant barotropic swirl velocity with maximum swirl speeds of 50 cm/s at a diameter of 80 km calculated by matching geostrophic velocity profiles with shipboard ADCP profiles (Martin et al., 1998). These authors found the eddy to have a downward distortion of density surfaces throughout the 2800 m water column below the center of the lens. Martin et al. (1998) suggest the eddy was produced by an instability on the NAC, perhaps topographically induced by the Hatton Bank, and that its core formed from Eastern North Atlantic Water created by deep winter mixing. Read and Pollard (2001) found another anticyclone near 59.5°N 21.0°W, which remained quasi-stationary from mid-April 1998 to the end of October 1998. They think it had a formation similar to the PRIME eddy and suggest that as the subpolar gyre contracted in 1996–1998 (Bersch et al., 1999) warm salty water penetrated the basin concentrated in large long-lived eddies. Our anticyclone AC1 is around 500 km southwest of these others, and might have translated southwestward from a possible formation site farther east off the Hatton Bank. However, a long southwestward translation appears to be inconsistent with the quasi-stationary behavior of these intense anticyclones. It seems more plausible that AC1 could have formed where it was observed by a westward meander of the NAC, which flows northeastward over the deeper part of the Basin (east of AC1) as indicated by non-looping floats.

As in the NAC region farther southwest, there appear to be several instances in the Iceland Basin of anticyclones coexisting alongside cyclones forming what look like dipoles (not shown). In March and April 1999 AC2 and C15 were located near 59°N 20°W, although AC2 moved away from C15 after a short while. Another dipole, C6 and AC13, occurred in the same months near 55°N 30°W. A third dipole, AC38 and C47, occurred in May 1999 near 60°N 24°W.

A few eddies were observed in the Rockall Trough, but detailed float tracking in this region was difficult due to the blocking of acoustic signals by the shallow topography of the Rockall Plateau. Therefore some large gaps occur in float trajectories in this region.

3.3. Irminger basin

On the western side of the Reykjanes Ridge four anticyclones (AC18, AC17, AC16, AC10) translated northeastward at around 2.1 cm/s ($\pm$0.4 cm/s) following the direction of the general circulation there (Figs. 2 and 5). In contrast to these, cyclone C1, which had 17.5 loops (the most of any cyclone) and was tracked for 5.5 months, cut northwestward across the entrance to the Irminger Basin at 2.2 cm/s. Although this direction is consistent with the self-advection velocity of a cyclone on a beta plane (Nof, 1981, 1983; Cushman-Roisin et al., 1990), the speed seems a little faster than typical, which could mean that background flow in that direction advected the eddy or that it was part of a self-advecting dipole. The important result is that this cyclone indicates an eddy shortcut across the southern part of the basin, one that short-circuits the dominant counter-clockwise boundary-following path around the northern part of the basin as indicated by most floats and the anticyclones (see also Lavender et al., 2000).

3.4. West European Basin

South of 53°N (roughly) the mean circulation estimated from floats in the eastern basin is much weaker than the general circulation in the NAC as it flows across the Ridge, around the Iceland Basin and into the Irminger Basin. The circulation in the West European Basin estimated from floats is difficult to characterize simply, but looks like sluggish zonal flows going in different directions at different latitudes with little net meridional flow (Bower et al., 2002; Fig. 6). Most eddies in this region, including both cyclones and anticyclones, had a southward component to their translation (Fig. 5), which may indicate a general southward flow in this region.

One striking result is that five floats looped in four different anticyclones (AC3, AC9, AC31, AC36) as they translated southwestward away from the Goban Spur located near 49°N 12°W (Fig. 12). The float trajectories in these eddies look rather similar to those in meddies tracked farther south (Käse and Zenk, 1996; Bower et al., 1997; Richardson et al., 2000; Paillet et al., 2002), and the translation velocity of the anticyclones is similar to that of meddies. The translation direction is consistent with the self-advection of an anticyclone on a beta plane.

The longest tracked of the meddy-like anticyclones (AC3) was by float 326, which looped for 16.5 months and translated 650 km, the farthest of any eddy. Although the loops of float 326 seemed to disappear near 47°N and also near 14°W (Fig. 12), small cusps near these locations indicate that the float continued to loop but that the swirl speed was smaller than the eddy translation speed. The three distinctive looping segments of the trajectory are labeled in Fig. 13A. For each segment, the float's position relative to the center of the eddy is shown in Fig. 13B, revealing the symmetrical circulation of the eddy. Immediately after launch, float 326 began looping with an average period of 5.5 days ($Ro = -0.24$) at diameters of 5–13 km, with the data indicating near solid body rotation (see Fig. 13C, Loops 1). This is around twice the period of rotation of newly formed meddies farther south (Richardson et al., 2000). The larger period of Loops 2 (10 days; Fig. 13C) could be caused by temporal changes in AC3 as implied by the irregular-shaped loops located between Loops 1 and 2 (Fig. 13A), which indicate that the normal eddy circulation was disrupted then. Float 326 looped 42 times as it translated southwestward at 1.5 cm/s, the same speed as the other long-tracked anticyclone in this group (AC9). Maximum swirl speeds measured by float 326 were 15 cm/s, approximately half that of newly formed meddies farther south. Temperatures in the central region of AC3 ($<$15 km diameter) near a depth of 900 m were greater than 9.4 °C in agreement with CTD measurements at the float launch that indicated warm saline water adjacent to the continental slope (Fig. 14). The warm core can be clearly seen in Fig. 13D. The

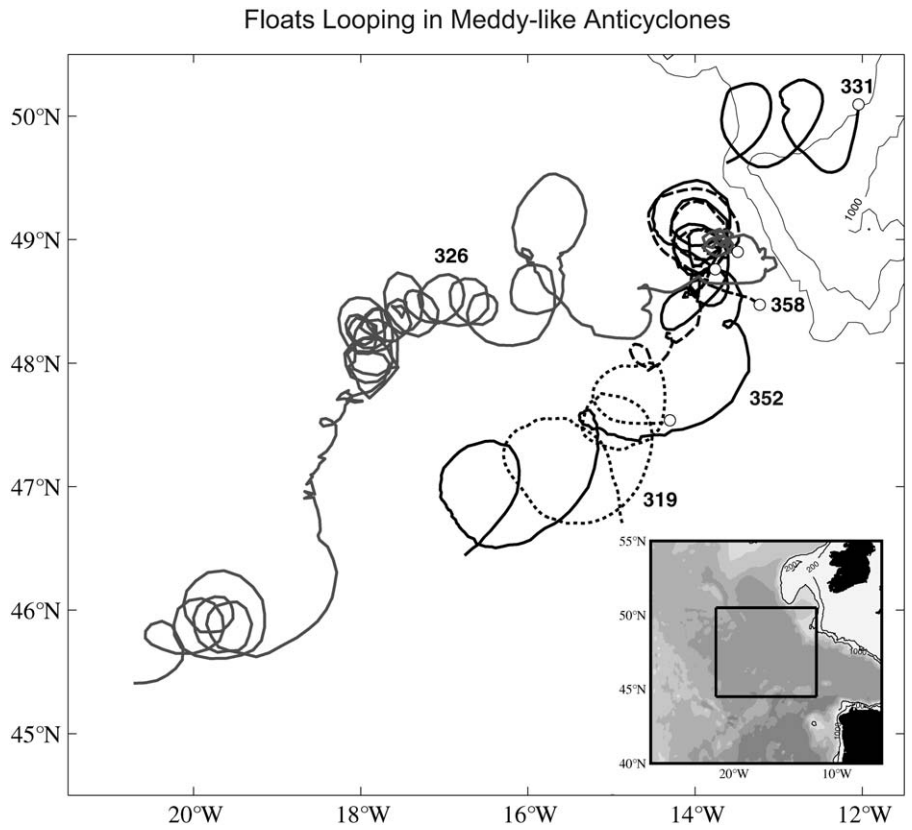

Fig. 12. Floats looping in four anticyclones, three of which translated southwestward away from the eastern boundary near the Goban Spur (49°N 12°W), float 326 in AC3, floats 352 and 358 in AC9, float 319 in AC31, and float 331 in AC36. These could have been weak meddies formed from remnants of warm salty Mediterranean Water advected northward along the eastern boundary. A possible formation mechanism is the sharp direction change of the boundary at the Goban Spur near 49°N 13°W seen in the upper right of this figure.

higher temperatures (~8.9 °C) measured at radii greater than ~22 km are principally from the third main set of loops (Loops 3, at ~19.5°W 46°N) and could be due to entrainment of warmer waters from outside the eddy or possibly from merging with another anticyclone.

Two floats, 352 and 358, were caught and looped in AC9, float 352 for 8.6 months. Float 358 measured a looping period of 6.5 days ($Ro = -0.21$) for some relatively small loops around 15 km in diameter. Float 319 looped three times in AC31, overlying the loops of float 352 (AC9) but 9 months earlier. One other anticyclone, AC36, was measured by float 331 on the northern edge of the Goban Spur but only for 2.5 loops. Floats started looping in these four anticyclones during December 1996, March, June and November 1997, suggesting a formation rate of at least 3–4 eddies per year in this region. Largest loops in AC9 and AC31 suggest these anticyclones have diameters of around 100 km.

We speculate that these anticyclones could have formed from a northward flow of water along the eastern boundary (see Pingree and Le Cann, 1989, 1990), at the sharp change in direction experienced at the Goban Spur, although there is little evidence from floats for a persistent northward boundary current. The apparent similarity of the anticyclone float trajectories to meddy float trajectories, the anomalously warm water observed in the core

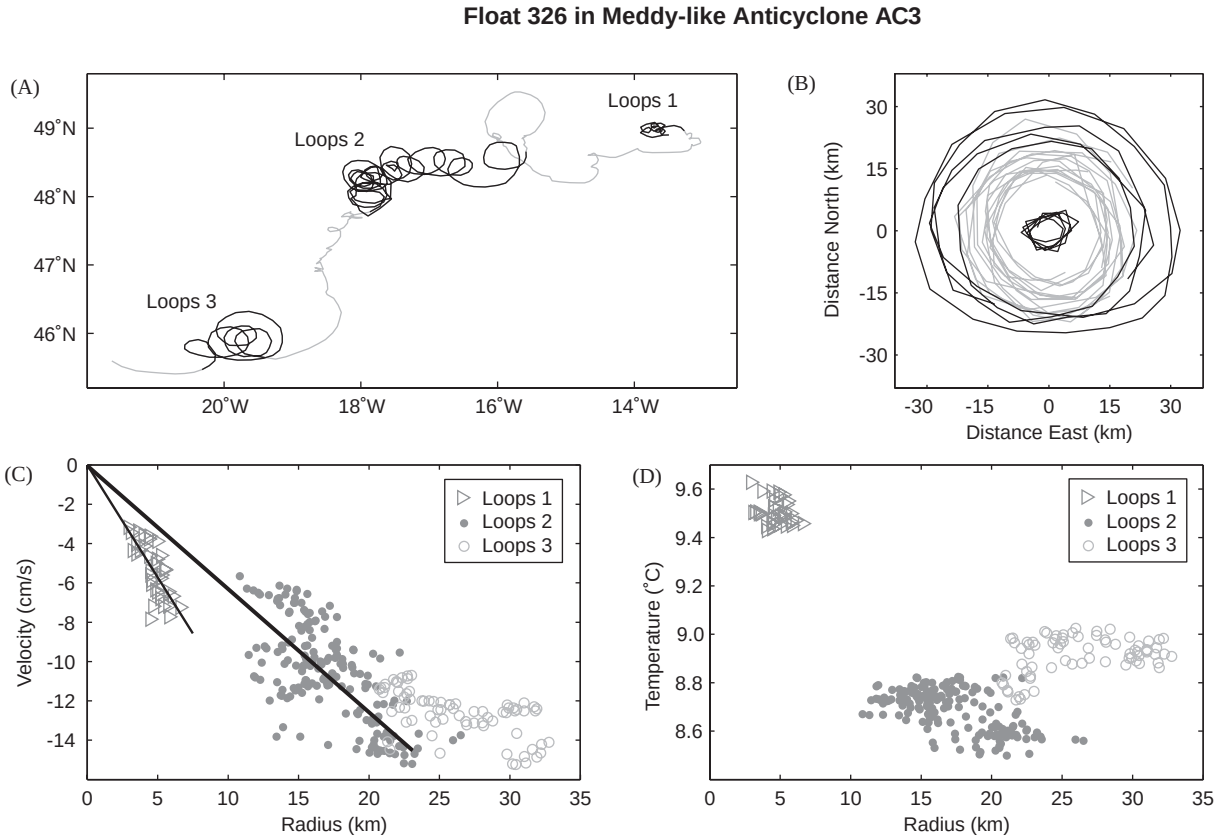

Fig. 13. Eddy AC3, a meddy-like eddy in the West European Basin, as measured by float 326: (A) float track with main looping parts used for this analysis shown in black; (B) float position relative to the eddy center as calculated by subtracting the mean eddy position from the float position; Loops 1 (smallest diameter) and 3 are black, Loops 2 are gray; (C) variation of swirl velocity with radius, with lines of constant period 5.5 days (thin black through Loops 1) and 10 days (thick black through Loops 2), indicating near solid body rotation at different times; (D) variation of temperature with radius. Loops 1 were centered near a depth of 920 m, Loops 2 near 1050 m and Loops 3 near 1000 m.

region of the anticyclones, and the slower core rotation rate and slower peak swirl speeds suggest that these anticyclones might be weaker versions of meddies. Without additional measurements we do not know if these eddies are subsurface lenses like meddies or are surface-intensified eddies perhaps like slope water eddies (swoddies) that have been observed to form near the eastern boundary farther south (44–46°N) in the Bay of Biscay (Pingree and Le Cann, 1992a, b). We tried to resolve this issue using Modular Ocean Data Assimilation System (MODAS) sea-surface height fields with float trajectories superimposed, but results were not conclusive because meddies cannot be easily distinguished from other anticyclonic eddies in the sea-surface height fields (see http://www.whoi.edu/science/PO/people/abower). The only information we have about the vertical structure of the velocity of these anticyclones is from Acoustic Doppler Current Profiler (ADCP) profiles made at the time float 326 was launched and began looping near its launch site in AC3. The ADCP velocity profiles near float 326 are somewhat noisy (presumably due to near inertial and baroclinic tidal motions), but subsurface, anticyclonic velocity maxima occur in the depth range of the Mediterranean Water (K. Donohue, 2003 pers. comm.); the best example is the velocity

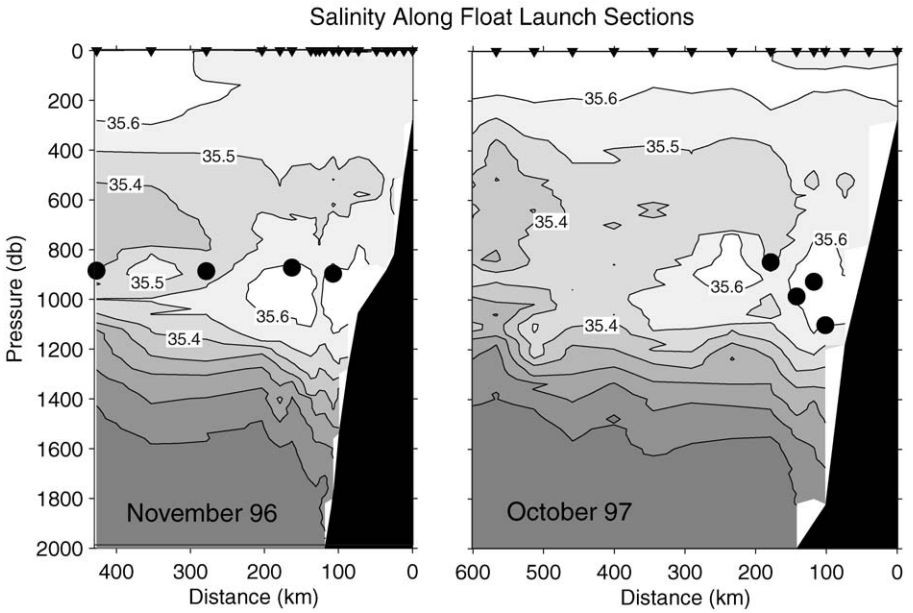

Fig. 14. Vertical sections of salinity measured off the Goban Spur in November 1996 (Knorr cruise 147) and October 1997 (Knorr cruise 154) courtesy of Ruth Curry and Mike McCartney. The sections show high salinity (>35.6) Mediterranean Water near the eastern boundary at 1000 m and the launch locations of floats shown by black dots. In the November 1996 section the second float from the right (326) looped near where it was launched in AC3. The right-hand float (331) translated northward around 100 km and began looping in AC36. In the October 1997 section the two middle floats (352, 358) translated 100 km northwestward and began looping in AC9. Thus, four of the five floats that were launched into the high salinity (>35.6) water near the eastern boundary at the Goban Spur began looping in meddy-like eddies.

profile at station 177 just east of where float 326 was launched and where it looped in AC3 (Fig. 15). Since these velocity maxima are larger than the near-surface velocities of the profiles, we tentatively conclude that at least initially AC3 is a subsurface lens, not a surface-intensified eddy.

The hydrographic measurements found traces of warm and salty water of Mediterranean origin near the Goban Spur that must have traveled northward along the eastern boundary (see Harvey, 1982). Presumably this water was entrained into the anticyclones at their formation as measured by warm float temperatures whether the eddies were lens-like or surface-intensified. Thus these eddies are inferred to bleed remnants of the Mediterranean Water away from the eastern boundary and transport this anomalously warm and salty water southwestward into the central and western parts of the West European Basin.

4. Discussion and summary

RAFOS float trajectories were used to identify discrete eddies and to describe their distribution, movement and characteristics. Eddies were found throughout the ACCE float region and occupy around 15% of the area as estimated by the percentage of looping records. Many eddies translated at 2–3 cm/s in the direction of the North Atlantic Current (NAC) as it crossed the Mid-Atlantic Ridge and flowed counter-clockwise around the Iceland Basin, westward over the Reykjanes Ridge, and into the Irminger Basin. The implication is that the background flow field generally advected the eddies and that eddy self-advection was small in comparison. One interesting eddy cut northwestward across the entrance to the Irminger Basin, short-circuiting the more typical counter-clockwise circulation around this basin.

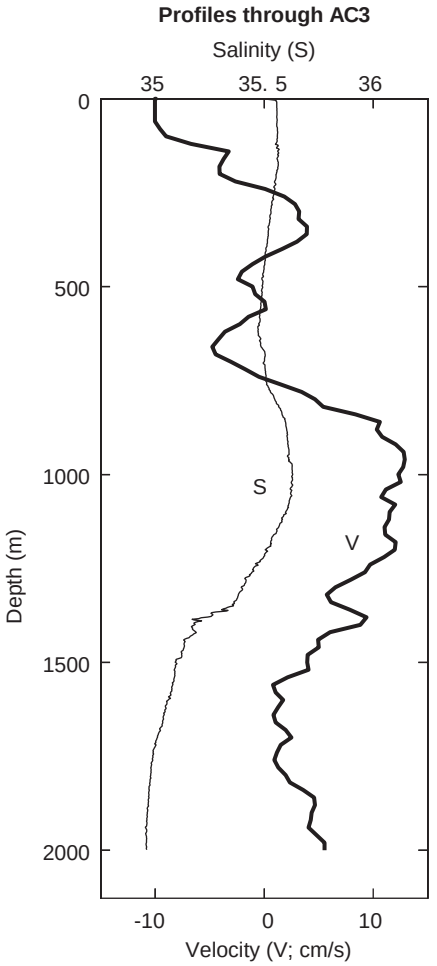

Fig. 15. Profiles of velocity (dark line) and salinity (light line) at 48.9°N 13.1°W (Fall 1996) just east of where float 326 was launched (and looped) in AC3 (courtesy of Kathy Donohue). The velocity profile is the velocity component in the direction of the mean velocity near 1000 m (260°). The maximum velocity of around 12 cm/s is centered near a depth of 1000 m and coincides with the maximum of salinity which is greater than 35.6.

Four anticyclones, which formed near the eastern boundary at the Goban Spur, translated generally southwestward at around 1.5 cm/s. In this region the mean current is much slower than that in the vicinity of the NAC (as estimated from all available floats), therefore the southwestward velocity of these eddies may be due to self-advection. Hydrographic measurements near the float deployments and warm float temperatures suggest that these anticyclones could contain a lens of warm salty water that had been advected northward along the eastern boundary, and therefore these eddies could be weak meddies. If true, these would be the northernmost observed meddies. The velocity profiles near float 326 in AC3 are consistent with this interpretation. These anticyclones are inferred to advect the remnants of Mediterranean Water away from the boundary and into the central and western parts of the basin.

A few energetic eddies remained quasi-stationary for long periods of time near where the NAC crossed the Mid-Atlantic Ridge, which appears by non-looping float trajectories to be preferentially over the Charlie Gibbs (52°N) and Faraday (50°N) Fracture Zones. We hypothesize that the NAC is constrained by sea floor topography in this region to form quasi-stationary meanders in which are embedded quasi-stationary eddies. An anticyclone in the central Iceland Basin remained quasi-stationary for 14 months, about 500 km southwest of where other quasi-stationary anticyclones have previously been observed. It is possible that this anticyclone formed from a westward meander of the NAC at the location it was discovered. Why it remained stationary is as yet unknown.

In this analysis, we found that cyclonic and anticyclonic eddies were observed with more or less equal frequency in the northern two quadrants of the study region (i.e. in the subpolar region north of 54°N), but cyclones were more prevalent in the southwestern quadrant, and anticyclones in the southeastern quadrant (see Fig. 3). Paillet (1999) observed a similar west-to-east increase in the relative abundance of anticyclones in his study of 162 Central Water vortices (100–700 m) in the region that overlaps with our study area. In the most general terms, instabilities of the large-scale currents such as the Gulf Stream or North Atlantic Current generate equal numbers of cyclones and anticyclones. Theoretical and numerical studies of the evolution of eddies in the ocean suggest that anticyclonic eddies will persist longer than cyclones because the former tend to merge, while the latter split into smaller (and presumably shorter-lived) eddies (Cushman-Roisin and Tang, 1990; Nof, 1991).

In the present study, we suspect that the distribution of cyclones and anticyclones is more related to the dominance of certain formation processes in different regions. We suggest that the abundance of anticyclonic eddies in the south-eastern region is related to the formation of meddy-like features along the eastern boundary, either by injection and geostrophic adjustment of the less-stratified Mediterranean Water into the more-stratified open ocean (McWilliams, 1985), or by separation of an anticyclonic shear layer at a sharp bathymetric corner (D'Asaro, 1988; Bower et al., 1997). Both processes favor anticyclonic eddy formation. Paillet (1999) came to the same conclusion based on the observations of preferential formation of anticyclonic eddies from the poleward eastern boundary current (Pingree and Le Cann, 1993). The predominance of cyclones in the southwest is not as clear, however we point out that many of the floats analyzed here were launched in the North Atlantic Current just upstream of the Mid-Atlantic Ridge, and the float tracks indicate the presence of a semi-permanent southward (cyclonic) meander of the NAC in the same vicinity. Thus the larger number of cyclonic eddies observed here may be due mostly to a bias in the sampling, and is representative of a specific area.

Acknowledgements

This is contribution 10907 from the Woods Hole Oceanographic Institution. Funds for this research were provided by National Science Foundation grants OCE-9531877 to WHOI and OCE-9906775 to URI. This work was also supported by a grant from the WHOI Associates. Much of the research was accomplished during a visit to WHOI by Deb Shoosmith, which was made possible through a student exchange supported by the School of Ocean and Earth Science, Southampton University and WHOI. Heather Furey and Sandy Anderson-Fontana tracked the ACCE RAFOS floats. Heather Furey generated many of the figures and the appendices. Ruth Curry and Mike McCartney generously provided the CTD data used in Fig. 14, and Kathy Donohue provided plots of the ADCP data, one of which was shown in Fig. 15.

Appendix A. Cyclones

Eddy	Float ID	Dates tracked (mmddyy)		Number of days tracked	Mean depth (m)	Mean temp (°C)	Number of loops	Looping period (days)	Rossby number (*Ro*)	Mean diam (km)	Mean swirl speed (cm/s)	Mean velocity (cm/s)		Mean location	
		Start	End									*U*	*V*	°N	°W
C1	421	012299	070899	168	571	3.9	17.5	9.6	0.12	29	11	−1.7	1.4	57.1	39.3
C2[a]	360	123197	082898	241	530	4.2	13.5	17.9	0.07	56	11	0.9	−1.4	51.2	34.3
C2	400	062898	082398	88	546	4.7	2.6	33.8	0.04	109	12			50.3	32.8
C3	540	040799	091499	161	59	7.1	12.5	12.9	0.09	30	8	−0.5	−0.8	54.4	33.1
C4	544	020899	072799	170	574	7.2	11.5	14.8	0.08	69	17	1.6	−0.4	51.8	21.5
C4	537	021499	040699	52	497	7.1	3.5	14.9	0.08	65	16	9.6	0.3	52.3	21.7
C4	558	022099	032499	33	482	7.4	2.2	15.0	0.08	75	18			52.5	22.5
C5	422	122497	040298	100	504	4.5	11.0	9.1	0.14	34	14	2.1	−0.2	51.3	38.0
C6	535	033099	062599	88	90	6.9	10.5	8.4	0.14	23	10	−0.5	0.4	55.4	30.6
C7	557	091799	122699	101	62	6.8	10.0	10.1	0.12	24	9	−0.6	1.6	55.9	36.4
C8	547	072499	091799	56	138	7.0	9.0	6.2	0.19	43	25	−3.5	−0.9	56.7	35.2
C9	358	022699	101899	235	1156	6.2	8.0	29.4	0.05	44	5	−0.6	−0.4	47.8	16.8
C10	566	072598	082398	30	94	6.0	7.5	4.0	0.31	7	7	−0.2	1.1	53.1	37.1
C11	419	032999	010199	218	970	6.4	7.0	31.1	0.04	63	7	0.3	−0.4	46.9	18.8
C12[b]	428	102397	031398	142	548	4.7	6.7	21.2	0.06	73	13	1.9	0.3	51.1	31.3
C12	479	121897	040298	106	438	5.1	8.2	12.9	0.10	47	13	1.2	−0.7	51.1	30.6
C12	480	010698	033098	84	443	5.3	5.0	16.8	0.08	65	14	0.6	0.0	51.0	30.5
C13	363	061798	082498	69	846	6.0	6.5	10.6	0.11	33	11	0.7	3.2	56.8	20.4

Appendix A. *Continued*

Eddy	Float ID	Dates tracked (mmddyy)		Number of days tracked	Mean depth (m)	Mean temp (°C)	Number of loops	Looping period (days)	Rossby number (*Ro*)	Mean diam (km)	Mean swirl speed (cm/s)	Mean velocity (cm/s)		Mean location	
		Start	End									*U*	*V*	°N	°W
C14	328	043098	072198	83	904	5.8	4.5	18.4	0.06	56	11	−0.3	0.6	61.4	16.5
C15	552	022299	041499	52	569	7.7	4.5	11.6	0.10	68	21			59.6	19.5
C16	354	050899	091399	129	1008	8.9	4.0	32.3	0.04	40	5	−0.9	0.3	46.4	8.7
C17	448	110597	121397	40	316	4.8	4.0	10.0	0.13	36	13	4.2	−0.7	51.8	36.6
C18	559	040899	071499	98	698	8.0	3.5	28.0	0.05	71	9	0.0	−2.0	44.9	30.7
C19	563	072598	092998	68	238	5.9	3.5	19.4	0.07	57	11	1.6	−1.6	51.9	36.6
C20	364	052899	082699	91	884	6.4	3.0	30.3	0.05	60	7	−1.2	2.3	46.7	22.1
C21	542	091098	102498	45	192	6.2	3.0	15.0	0.09	45	11	2.8	1.0	51.1	34.8
C22	377	061298	072598	44	734	4.0	3.0	14.7	0.08	33	8	3.6	−0.6	52.7	29.7
C23	317	011297	022197	41	948	8.1	3.0	13.7	0.09	33	9			54.7	13.0
C24	416	010399	012799	25	818	6.8	3.0	8.3	0.14	15	7	−2.4	0.0	61.5	17.4
C25	427	060499	062399	20	530	5.6	3.0	6.7	0.17	18	10	−3.6	−3.2	59.4	29.4
C26	557	072799	081099	15	40	6.5	3.0	5.0	0.24	17	12			55.5	38.7
C27	558	102098	122698	68	520	7.2	2.7	25.2	0.05	57	8			48.8	29.2
C28	348	062999	081099	43	710	7.0	2.7	15.9	0.07	83	19			59.1	20.6
C29	368	051599	062399	40	856	5.2	2.6	15.4	0.08	56	14			57.0	23.5
C30	319	040598	062298	76	929	8.4	2.5	30.4	0.04	44	5			49.3	14.3
C31	428	061498	081298	60	590	4.9	2.5	24.0	0.05	56	8			54.5	23.5
C32	377	091698	102698	41	763	4.0	2.5	16.4	0.08	33	7			54.9	27.1
C33	549	051299	061999	39	330	6.5	2.5	15.6	0.08	91	21			53.0	23.4
C34	537	072999	082599	28	563	9.2	2.5	11.2	0.11	60	20			55.3	10.9
C35	534	081098	090198	23	492	6.1	2.5	9.2	0.15	25	10			46.9	35.1
C36	538	122299	010400	14	113	6.3	2.5	5.6	0.22	17	11			54.0	37.8
C37	356	100697	110697	32	721	3.6	2.3	13.9	0.09	38	10			53.2	39.3
C38	317	100997	111297	35	937	7.0	2.2	15.9	0.08	78	18			55.3	14.3
C39	317	060298	062098	19	1013	7.6	2.2	8.6	0.14	48	20			54.9	12.0
C40	541	081998	100198	44	453	6.7	2.1	21.0	0.06	105	18			48.9	36.1
C41	389	062098	090498	77	555	4.6	2.0	38.5	0.03	64	6			55.7	27.9
C42	554	092798	121198	76	690	6.9	2.0	38.0	0.04	119	11			44.9	32.1
C43	377	030398	041898	47	712	3.9	2.0	23.5	0.05	17	3			53.3	32.6
C44	459	110597	121097	37	423	6.3	2.0	18.5	0.07	80	16			50.3	36.8
C45	476	100198	110498	35	664	6.3	2.0	17.5	0.06	65	13			60.2	24.0
C46	550	072399	081799	26	59	7.6	2.0	13.0	0.09	76	21			63.6	31.3
C47	347	042999	050999	11	510	7.0	2.0	5.5	0.21	14	9			60.4	23.1
Mean				72	558	6.2	4.7	16.8	0.10	51	12	0.5	0		
Standard deviation				56	290	1.3	3.6	8.8	0.06	26	5	2.7	1.3		

[a]C2 was tracked for 267 days.
[b]C12 was tracked for 162 days.

Appendix B. Anticyclones

Eddy	Float ID	Dates tracked (mmddyy)		Number of days tracked	Mean depth (m)	Mean temp (°C)	Number of loops	Looping period (days)	Rossby number (*Ro*)	Mean diam (km)	Mean swirl speed (cm/s)	Mean velocity (cm/s)		Mean location	
		Start	End									*U*	*V*	°N	°W
AC1[a]	569	121698	111699	336	240	8.0	46.0	7.3	−0.16	47	23			56.7	27.8
AC1	389	100398	011699	106	608	5.5	8.0	13.3	−0.09	58	16			56.6	28.9
AC1	576	081599	092899	45	427	6.9	2.8	16.1	−0.08	82	19			56.3	27.6
AC2	413	041199	100899	181	827	7.9	43.0	4.2	−0.28	17	14	−0.7	0.7	59.6	21.5
AC3[b]	326	120396	041898	502	1007	8.9	42.0	12.0	−0.11	33	10	−1.2	−0.9	48.0	17.0
AC4	538	030299	072899	149	63	7.2	36.0	4.1	−0.29	19	17	−1.5	−1.1	56.1	34.4
AC5	546	031799	062899	104	259	6.4	22.0	4.7	−0.26	13	10	0.6	2.2	53.6	28.9
AC6[c]	418	102897	072598	271	714	5.8	15.0	18.1	−0.07	61	12			50.1	35.1
AC6	413	103197	031398	134	700	5.6	4.5	29.8	−0.04	109	13			50.1	35.2
AC6	400	102197	062898	251	662	5.5	13.0	19.3	−0.07	77	14			50.2	35.1
AC7	546	091399	112299	71	226	7.0	11.0	6.5	−0.19	12	7	−1.0	0.2	54.4	29.7
AC8	318	092797	010598	101	1059	6.8	10.5	9.6	−0.13	22	8	−1.8	2.0	55.5	21.0
AC9[b]	352	111897	080598	261	1028	8.6	10.0	26.1	−0.05	57	8	−1.0	−1.1	48.0	14.8
AC9	358	111597	031898	124	1126	8.0	9.0	13.8	−0.09	33	9	−1.0	−0.6	48.7	14.1
AC10	572	060599	081499	71	50	7.5	9.8	7.2	−0.16	41	21	2.0	1.4	63.1	32.3
AC11	429	081299	101999	69	660	5.6	9.5	7.3	−0.16	20	10	−3.0	−4.6	56.2	32.5
AC12	564	072498	091098	50	264	6.7	8.0	6.2	−0.20	21	13	0.0	−2.7	52.4	37.4
AC12	537	072598	090898	47	128	7.0	7.0	6.7	−0.19	37	20	−0.2	−3.5	52.4	37.3
AC12	553	072598	090798	46	184	6.9	8.0	5.8	−0.22	23	14	−0.4	−3.0	52.4	37.5
AC13	535	020399	032599	51	191	6.6	7.5	6.8	−0.18	26	14	−0.2	2.5	54.5	30.1
AC14	346	111498	030999	116	878	7.5	6.5	17.8	−0.07	49	10	1.9	−0.7	49.1	21.4
AC15	564	011899	070599	169	575	6.6	6.0	28.2	−0.05	122	16			50.9	31.4
AC16	425	082798	110698	72	550	5.4	5.5	13.1	−0.09	37	10	1.7	2.3	60.5	32.5
AC17	356	060398	101598	135	728	3.6	5.0	27.0	−0.04	59	8	0.5	1.0	56.1	38.3
AC18	349	091597	121797	94	758	3.5	5.0	18.8	−0.06	30	6	1.4	1.5	55.1	39.2
AC19	377	033099	052499	56	952	5.5	5.0	11.2	−0.11	54	18	−1.5	−1.2	58.4	24.9
AC20	561	082299	091299	22	98	6.5	4.8	4.6	−0.25	25	20			59.4	34.6
AC21	355	102797	060398	220	731	6.8	4.5	48.9	−0.03	89	7			47.7	29.8
AC22	364	030698	041998	45	995	8.1	4.5	10.0	−0.13	31	11	−1.5	−2.4	51.7	16.3
AC23	364	103098	032099	142	977	7.1	4.0	35.5	−0.04	74	8	−0.6	−1.1	47.3	23.8
AC24	348	123198	030399	63	655	6.4	4.0	15.8	−0.08	49	10	2.2	1.4	56.3	24.7
AC25	317	082198	100898	49	1020	8.2	4.0	12.3	−0.10	79	24	−0.7	1.0	54.7	12.1
AC26	317	050498	052898	25	1055	8.8	4.0	6.2	−0.20	30	18	2.4	0.4	55.4	13.3
AC27	459	122597	032298	88	344	6.4	3.5	25.1	−0.05	50	7	1.5	0.8	51.9	34.0
AC28	364	110597	010198	58	975	8.2	3.5	16.6	−0.08	38	8	−1.8	2.3	51.1	17.5
AC29	349	012899	031599	47	1024	3.1	3.3	14.2	−0.09	32	8	0.1	−0.5	56.6	38.6
AC30	423	121098	042499	136	943	9.0	3.0	45.3	−0.03	118	10			44.8	22.7
AC31[b]	319	063097	101397	106	962	8.9	3.0	35.3	−0.04	86	9	−0.5	−1.1	47.4	15.1
AC32	546	071799	082999	44	316	6.8	3.0	14.7	−0.08	63	15			55.7	28.7
AC33	363	031699	041599	31	880	6.1	3.0	10.3	−0.11	45	16			61.8	20.3
AC34	324	120196	122996	29	902	8.7	3.0	9.7	−0.13	31	11			51.5	16.3
AC35	560	112298	121598	24	261	6.4	2.7	8.9	−0.14	42	17			52.8	28.5
AC36[b]	331	030797	052797	82	1000	9.4	2.5	32.8	−0.04	68	8			49.9	12.8
AC37	510	111998	012299	65	696	7.5	2.5	26.0	−0.05	76	11			45.8	34.3
AC38	355	042799	051999	13	664	7.1	2.5	5.2	−0.22	25	18			60.2	23.7
AC39	429	050798	071798	72	508	4.2	2.3	31.3	−0.04	39	5			53.5	29.9
AC40	360	072499	091799	56	685	5.5	2.3	24.3	−0.05	75	11			55.3	26.2
AC41	343	011299	031399	61	847	7.6	2.2	27.7	−0.05	102	13			51.0	21.1
AC42	547	103198	123098	61	508	6.3	2.0	30.5	−0.04	57	7			52.5	26.8
AC43	553	050999	062199	44	385	7.2	2.0	22.0	−0.05	93	15			57.6	28.0
AC44	561	042699	052699	31	351	5.9	2.0	15.5	−0.08	24	5			54.6	31.1
AC45	530	082399	091799	26	758	7.2	2.0	13.0	−0.09	112	31			58.9	21.3

Appendix B. *Continued*

Eddy	Float ID	Dates tracked (mmddyy)		Number of days tracked	Mean depth (m)	Mean temp (°C)	Number of loops	Looping period (days)	Rossby number (*Ro*)	Mean diam (km)	Mean swirl speed (cm/s)	Mean velocity (cm/s)		Mean location	
		Start	End									*U*	*V*	°N	°W
AC46	557	051099	060299	24	24	5.2	2.0	12.0	−0.10	94	28			57.9	40.6
AC47	420	012399	021099	19	734	6.1	2.0	9.5	−0.12	37	13			58.5	28.7
AC48	547	112099	113099	11	85	6.5	2.0	5.5	−0.21	28	18			60.0	33.9
AC49	540	123099	010800	10	26	5.9	2.0	5.0	−0.25	19	13			53.8	39.3
Mean				95	612	6.7	7.9	16.3	−0.11	52	13	−0.1	−0.2		
Standard Deviation				90	334	1.4	10.2	10.8	0.07	29	6	1.4	1.9		

[a]Quasi-stationary, Iceland Basin, AC1 was tracked for 439 days.
[b]Meddy-like anticyclones are AC3, AC9, AC31, and AC36; AC9 was tracked for 264 days.
[c]Quasi-stationary, NAC, AC6 was tracked for 278 days.

References

Anderson-Fontana, S., Lazarevich, P., Perez-Brunius, P., Prater, M., Rossby, H.T., Zhang, H.-M., 2001. RAFOS Float Data Report of the Atlantic Climate Change Experiment (ACCE) 1997–2000. Graduate School of Oceanography, University of Rhode Island Technical Report, Reference 01-4, 112pp.

Bersch, M., Meinke, J., Sy, A., 1999. Interannual thermocline changes in the North Atlantic 1991–1996. Deep-Sea Research II 46, 55–75.

Bower, A.S., Armi, L., Ambar, I., 1997. Lagrangian observations of Meddy formation during a Mediterranean undercurrent seeding experiment. Journal of Physical Oceanography 27 (12), 2545–2575.

Bower, A.S., Richardson, P.L., Hunt, H.D., Rossby, T., Prater, M.D., Zhang, H.-M., Anderson-Fontana, S., Perez-Brunius, P., Lazarevich, P., 2000. Warm-water pathways in the Subpolar North Atlantic: an overview of the ACCE RAFOS float programme. International WOCE Newsletter 38, 14–16.

Bower, A.S., Le Cann, B., Rossby, T., Zenk, W., Gould, J., Speer, K., Richardson, P.L., Prater, M.D., Zhang, H.-M., 2002. Directly measured mid-depth circulation in the northeastern North Atlantic Ocean. Nature 419 (6907), 603–607.

Byrne, D., Gordon, A., Haxby, W., 1995. Agulhas eddies: a synoptic view using Geosat ERM data. Journal of Physical Oceanography 25, 902–917.

Cushman-Roisin, B., Tang, B., 1990. Geostrophic turbulence and emergence of eddies beyond the radius of deformation. Journal of Physical Oceanography 20, 97–113.

Cushman-Roisin, B., Chassignet, E.P., Tang, B., 1990. Westward motion of mesoscale eddies. Journal of Physical Oceanography 20, 758–768.

D'Asaro, E., 1988. Generation of submesoscale vortices: a new mechanism. Journal of Geophysical Research 93, 6685–6694.

Dutkiewicz, S., Rothstein, L., Rossby, T., 2001. Pathways of cross-frontal exchange in the North Atlantic Current. Journal of Geophysical Research 106 (C11), 26,917–26,928.

Fratantoni, D.M., 2001. North Atlantic surface circulation during the 1990's observed with satellite-tracked drifters. Journal of Geophysical Research 106 (C10), 22,067–22,093.

Furey, H.H., Bower, A.S., Richardson, P.L., 2001. Warm water pathways in the Northeastern North Atlantic, ACCE RAFOS Float Data Report, November 1996–November 1999. Woods Hole Oceanographic Institution Technical Report WHOI-2001-17. Woods Hole, MA, 02543.

Harvey, J., 1982. Theta–*S* relationship and water masses in the eastern North Atlantic. Deep-Sea Research 29, 1021–1033.

Heywood, K.J., McDonagh, E.L., White, M.A., 1994. Eddy kinetic energy of the North Atlantic subpolar gyre from satellite altimetry. Journal of Geophysical Research 99 (C11), 22,525–22,539.

Käse, R.H., Zenk, W., 1996. Structure of the Mediterranean Water and Meddy characteristics in the northeastern Atlantic. In: Krauss, W. (Ed.), Warm water sphere of the North Atlantic Ocean. Gebruder Borntraeger, Berlin, pp. 365–395.

Lavender, K.L., Davis, R.E., Owens, W.B., 2000. Direct velocity measurements describe a new circulation regime in the Labrador and Irminger Seas. Nature 407, 66–69.

Martin, A.P., Wade, I.P., Richards, K.J., Heywood, K.J., 1998. The PRIME Eddy. Journal of Marine Research 56, 439–462.

McCartney, M.S., Mauritzen, C., 2001. On the origin of the warm inflow to the Nordic Seas. Progress in Oceanography 51, 125–214.

McWilliams, J.C., 1985. Submesoscale, coherent vortices in the ocean. Reviews of Geophysics 23 (2), 165–182.

Nof, D., 1981. On the β-induced movement of isolated baroclinic eddies. Journal of Physical Oceanography 11, 1662–1672.

Nof, D., 1983. On the migration of isolated eddies with application to Gulf Stream rings. Journal of Marine Research 41, 399–425.

Nof, D., 1991. Fission of single and multiple eddies. Journal of Physical Oceanography 21, 40–52.

Paillet, J., 1999. Central water vortices of the Eastern North Atlantic. Journal of Physical Oceanography 29, 2487–2503.

Paillet, J., Le Cann, B., Carton, X., Morel, Y., Serpette, A., 2002. Dynamics and evolution of a Northern Meddy. Journal of Physical Oceanography 32, 55–79.

Pingree, R.D., Le Cann, B., 1989. Celtic and Armorican slope and shelf residual currents. Progress in Oceanography 23, 303–338.

Pingree, R.D., Le Cann, B., 1990. Structure, strength and seasonality of the slope currents in the Bay of Biscay region. Journal of the Marine Biological Association of the United Kingdom 70, 857–885.

Pingree, R.D., Le Cann, B., 1992a. Anticyclonic Eddy X91 in the Southern Bay of Biscay, May 1991 to February 1992. Journal of Geophysical Research 97, 14,353–14,367.

Pingree, R.D., Le Cann, B., 1992b. Three anticyclonic Slope Water Oceanic eDDIES (SWODDIES) in the Southern Bay of Biscay in 1990. Deep-Sea Research 39, 1147–1175.

Pingree, R.D., Le Cann, B., 1993. A shallow meddy (a smeddy) from the secondary Mediterranean salinity maximum. Journal of Geophysical Research 98, 20,169–20,185.

Read, J.R., Pollard, R.T., 2001. A long-lived eddy in the Iceland Basin 1998. Journal of Geophysical Research 106, 11,411–11,421.

Reid, J.L., 1978. On the middepth circulation and salinity field in the North Atlantic Ocean. Journal of Geophysical Research 83, 5063–5067.

Richardson, P.L., 1993. A census of eddies observed in North Atlantic SOFAR float data. Progress in Oceanography 31, 1–50.

Richardson, P.L., Garzoli, S.L., 2003. Characteristics of intermediate water flow in the Benguela Current as measured with RAFOS floats. Deep-Sea Research II 50 (1), 87–118.

Richardson, P.L., Bower, A.S., Zenk, W., 2000. A census of Meddies tracked by floats. Progress in Oceanography 45, 209–250.

Rossby, H.T., 1996. The North Atlantic Current and surrounding waters: at the crossroads. Reviews of Geophysics 34 (4), 463–481.

Rossby, T., Prater, M.D., Zhang, H.-M., Anderson-Fontana, S., Perez-Brunius, P., Lazarevich, P., Bower, A.S., Richardson, P.L., Hunt, H., 2000. Warm-water pathways in the Subpolar North Atlantic: some case studies. International WOCE Newsletter 38, 17–19.

Schouten, M.W., de Ruijter, W.P.M., van Leeuwen, P.J., Lutjeharms, J.R.E., 2000. Translation, decay, and splitting of Agulhas rings in the southeastern Atlantic Ocean. Journal of Geophysical Research 105, 21,913–21,925.

Wade, I.P., Heywood, K.J., 2001. Tracking the PRIME eddy using satellite altimetry. Deep-Sea Research II 48, 725–737.